Sparse 3D Array made from Nested Linear Array Branches for Underdetermined Source Localization

Shekhar Kumar Yadav, Graduate Student Member, IEEE and Nithin V. George, Member, IEEE
Department of Electrical Engineering, Indian Institute of Technology Gandhinagar, India
{yadav_shekhar, nithin}@iitgn.ac.in

***Abstract*—Non-uniform sparse arrays like nested arrays have the ability to estimate the direction-of-arrival (DOA) of more sources than the number of sensors. These arrays are designed in such a manner such that their difference coarray is hole free. Then, the increased degrees-of-freedom (DOF) of the coarray is utilized to perform underdetermined DOA estimation. In this paper, we extend the nested array configuration to three-dimensional geometry to cover the entire azimuth and elevation range. The proposed 3D sparse array is made from three orthogonal nested array branches and the final structure is composed of a direct sum of these three branches. We study the structure and geometry of the difference coarray of the proposed array and extend the coarray based DOA estimation algorithm to 3D arrays. We propose a computationally efficient way to construct the full rank coarray covariance matrix for 3D sparse arrays. We also derive the unconditional Cramer-Rao Bound (CRB) for 3D sparse array signal model. Simulation results show the effectiveness and advantages of the proposed 3D structure.**

***Index Terms*—Array Processing, 3D Nested Arrays, DOA estimation, Difference Coarray, Spatial Smoothing, MUSIC**

I. INTRODUCTION

Direction-of-arrival (DOA) estimation is considered of great importance in the area of array processing and finds application in numerous fields such as sonar, radar, wireless communication, acoustics, robot audition, massive MIMO etc. [1]. Conventional DOA estimation algorithms like MUSIC are capable of estimating the DOA of only $(N-1)$ sources using an array of N sensors. Recently, in [2], a configuration of non-uniform linear sparse arrays (called the nested arrays) was introduced along with a DOA estimation method that theoretically enables estimating $\mathcal{O}(N^2)$ number of sources using just N sensors [3]. Subsequently, many other linear sparse array configurations have been designed [4]–[8] which are also capable of performing underdetermined DOA estimation. In [9], the idea of nested arrays was extended to two dimensions (2D) to perform underdetermined DOA estimation in both the azimuth and elevation directions. Other 2D sparse arrays and techniques for underdetermined 2D DOA estimation [10]–[14] have also been proposed. Sparse arrays on moving platforms [15]–[17] have also been used for underdetermined DOA estimation.

The drawback of linear arrays is that they can only provide a coverage of 180° in the azimuth direction. Planar arrays provide a complete coverage of the azimuth direction but only a 90° coverage in the elevation direction. Three dimensional (3D) arrays have the ability to cover the entire azimuth and elevation range. In [18], a 3D coprime sparse array was introduced. In this paper, we introduce a form of 3D nested array and analyze the structure of its difference coarray. We then introduce an efficient technique to construct the coarray covariance matrix and extend the coarray based algorithm to perform underdetermined DOA estimation in the entire range of azimuth and elevation angles. We also derive the CRB for 3D sparse array signal model.

Notations: $(.)^H$, $(.)^*$ and $(.)^T$ denotes the conjugate transpose operator, the conjugate operator and the transpose operator respectively. $\mathbb{E}[.]$, $\odot$, $\otimes$ and $\|.\|_F$ represents the expectation operator, the Khatri-Rao product, the Kronecker product and the Frobenius norm respectively. $\mathbf{I}_N$ represents an identity matrix of size $N \times N$ and $\mathbf{0}_{N\times M}$ represents a zero matrix of size $N \times M$. $\cup$ represents the union operation.

II. PROPOSED ARRAY STRUCTURE

Let us consider a 3D grid with one corner lying at the origin and let the spacing between two consecutive grid points in the x, y and z directions be d_x, d_y and d_z, respectively. Let us now place non-uniform nested linear arrays [2] of the same configuration along the x, y and z axis with the first element of all the three nested arrays lying at the origin. A nested array (more precisely a two-level nested array) is designed as a concatenation of two ULAs: one inner and one outer. The inner ULA has N_1 sensors with a spacing of d_1 and the outer ULA has N_2 sensors with a spacing of $d_2 = (N_1+1)d_1$. So, the 3D co-ordinates of the sensors lying on the three axes are given by $(X_N, 0, 0) \cup (0, Y_N, 0) \cup (0, 0, Z_N)$ where

$$
\begin{aligned}
X_N \in &\{0, 1, \dots, N_1-1\}d_x \,\cup \\
&\{N_1, 2(N_1+1)-1, \dots, N_2(N_1+1)-1\}d_x \\
Y_N \in &\{0, 1, \dots, N_1-1\}d_y \,\cup \\
&\{N_1, 2(N_1+1)-1, \dots, N_2(N_1+1)-1\}d_y \\
Z_N \in &\{0, 1, \dots, N_1-1\}d_z \,\cup \\
&\{N_1, 2(N_1+1)-1, \dots, N_2(N_1+1)-1\}d_z
\end{aligned}
$$

We consider a uniform 3D grid which means that the grid spacing in all the directions is the same ($d_x = d_y = d_z$). The final co-ordinates of all the sensors in the the proposed 3D array is given as

$$(x_n, y_n, z_n), \forall\ x_n \in X_N, y_n \in Y_N \text{ and } z_n \in Z_N \tag{1}$$

This work is supported by the Department of Science and Technology, Government of India under the Core Grant Scheme (CRG/2018/002919) and TEOCO Chair of Indian Institute of Technology Gandhinagar.

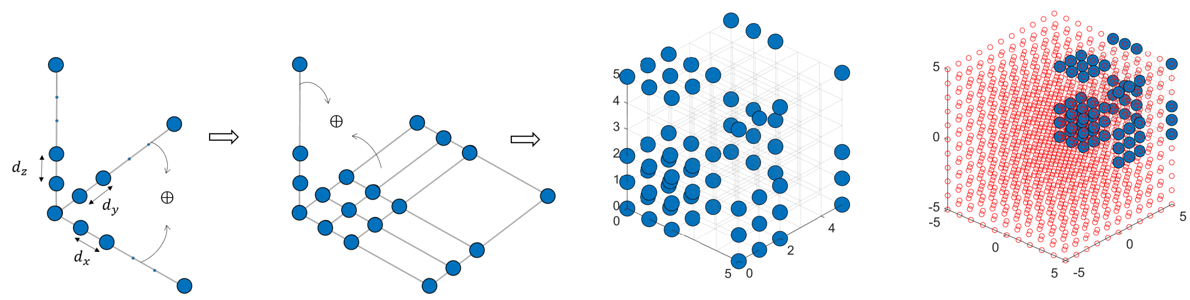

(a) (b) (c) (d)

Fig. 1. Structure of the proposed 3D array for $N_1 = N_2 = 2$. a) Shows the three branches of the 3D array, b) shows the intermediate structure formed by the direct sum of the nested arrays in the x and y axes, c) shows the final structure and d) shows the difference coarray of the proposed 3D array (red bubbles represent the coarray sensors) (note how the coarray is a completely filled uniform cube array).

These co-ordinates can be seen as the direct sum of X_N, Y_N and Z_N represented by $(X_N \oplus Y_N \oplus Z_N)$[1]. So, the total number of sensors in the proposed 3D nested array for a given N_1 and N_2 (that makes up the three nested branches of the 3D array) is $(N_1+N_2)^3$. Figure 1 shows the configuration of the proposed array for $N_1 = N_2 = 2$.

1) 3D Array Signal Model: Let $N = (N_1 + N_2)^3$ denote the total number of sensors in the proposed 3D nested array. And let $\mathbf{n}_n = [x_n, y_n, z_n]^T, n \in \{1, 2, \ldots, N\}$ denote the position vector of the n^{th} sensor. Now, let us consider L far-field narrowband and pairwise uncorrelated sources impinging on the array from directions given by the elevation and azimuth angle pairs $(\theta_l, \phi_l), l \in \{1, 2, \ldots, L\}$. The elevation angle in calculated down from the positive z-axis (has a range of $180°$) and the azimuth angle is calculated counter-clockwise from the positive x-axis (has a range of $360°$). The unit position vector pointing towards the DOA of the l^{th} source is given by $\mathbf{r}_l = [\sin\theta_l \cos\phi_l, \sin\theta_l \sin\phi_l, \cos\theta_l]^T$. Now, the signal collected by the array can be written as

$$\mathbf{x}(t) = \sum\nolimits_{l=1}^{L} s_l(t)\mathbf{a}(\theta_l, \phi_l) + \boldsymbol{\eta}(t) = \mathbf{A}\mathbf{s}(t) + \boldsymbol{\eta}(t), \quad (2)$$

where $\mathbf{s}(t)$ is an $L \times 1$ vector of source signal amplitudes and $\boldsymbol{\eta}(t)$ is a vector of zero mean gaussian sensor noise (each sensor is assumed to have uniform power of σ_η^2 and considered uncorrelated to the sources and each other). The steering matrix $\mathbf{A}$ can be written as [1] (λ is the wavelength of the signals)

$$\mathbf{A} = [\mathbf{a}(\theta_1, \phi_1), \mathbf{a}(\theta_2, \phi_2), \ldots, \mathbf{a}(\theta_L, \phi_L)]$$
$$\mathbf{a}(\theta_l, \phi_l) = \left[e^{-j\frac{2\pi}{\lambda}\mathbf{r}_l^T\mathbf{n}_1}, e^{-j\frac{2\pi}{\lambda}\mathbf{r}_l^T\mathbf{n}_2}, \ldots, e^{-j\frac{2\pi}{\lambda}\mathbf{r}_l^T\mathbf{n}_N}\right]^T$$

Now, the covariance matrix of the received signal is given as

$$\mathbf{R} = \mathbb{E}[\mathbf{x}\mathbf{x}^H] = \sum\nolimits_{l=1}^{L} p_l \mathbf{a}(\theta_l, \phi_l)\mathbf{a}^H(\theta_l, \phi_l) + \sigma_\eta^2 \mathbf{I}_N, \quad (3)$$
$$= \mathbf{A}\mathbf{P}\mathbf{A}^H + \mathbf{R}_{\boldsymbol{\eta}}, \quad (4)$$

where $\mathbf{P}$ and $\mathbf{R}_{\boldsymbol{\eta}}$ are the signal and noise covariance matrices respectively. For uncorrelated sources, $\mathbf{P} = \text{diag}(p_1, p_2, \ldots, p_L)$ where p_l represents the power of the l^{th} source. It is interesting to note that the elements in the array covariance matrix depend on the pairwise differences of the sensor locations as, from (3), its $(u, v)^{th}$ element is

$$[\mathbf{R}]_{uv} = \sum\nolimits_{l=1}^{L} p_l e^{-j\frac{2\pi}{\lambda}\mathbf{r}_l^T(\mathbf{n}_u - \mathbf{n}_v)} + \sigma_\eta^2 \delta(u - v), \quad (5)$$

So, the second-order statistics of the signal captured by the array depends on the pairwise differences of the actual sensor locations. A difference coarray can now be defined as a virtual array whose virtual sensors locations are given by the set $\mathbf{D} = \{(\mathbf{n}_u - \mathbf{n}_v), \forall\, u, v = 1, 2, \ldots, N\}$. There maybe redundancies in $\mathbf{D}$ owing to the same difference between two distinct pairs of sensor locations (shown in Figure 2). However, what is important is the fact that the number of virtual coarray sensors (also referred to as the DOF of the coarray) is of the order of $\mathcal{O}(N^2)$. Since, the proposed 3D array is made up of three linear nested array branches, its difference coarray depends on the coarray of its branches. The difference coarray of the nested array in the x-axis is a filled uniform linear array (ULA) [2] with $2N_2(N_1 + 1) - 1$ elements whose positions are given by the set $X_D = \{nd_x, n = -M, \ldots, M\}$ ($M = N_2(N_1 + 1) - 1$). Y_D and Z_D can be defined in a similar manner. Now, the coarray sensor positions of the entire 3D nested array is given by the direct sum $(X_D \oplus Y_D \oplus Z_D)$. This is because the coarray sensor locations are given by

$$(x_n, y_n, z_n) - (x_{n'}, y_{n'}, z_{n'}), \quad (6)$$
$$\forall\, x_n, x_{n'} \in X_N; y_n, y_{n'} \in Y_N \text{ and } z_n, z_{n'} \in Z_N$$
$$= (x_n - x_{n'}, y_n - y_{n'}, z_n - z_{n'}), \quad (7)$$
$$= (x_d, y_d, z_d), \quad \forall\, x_d \in X_D, y_d \in Y_D \text{ and } z_d \in Z_D. \quad (8)$$

Therefore, the difference coarray of the proposed 3D array is a contiguous uniform cube array with $D = |\mathbf{D}| = (2N_2(N_1 + 1) - 1)^3$ coarray sensors. The difference coarray for an array with $N_1 = N_2 = 2$ is shown in Figure 1(d) and as expected it has 1331 elements. It is noteworthy to highlight the increased DOF of the coarray compared to the actual array which is utilized for underdetermined DOA estimation.

[1]The direct sum of three abelian groups A, B and C is another abelian group $(A \oplus B \oplus C)$ consisting of all the ordered pairs $\{(a, b, c)\}$ where $a \in A, b \in B$ and $c \in C$.

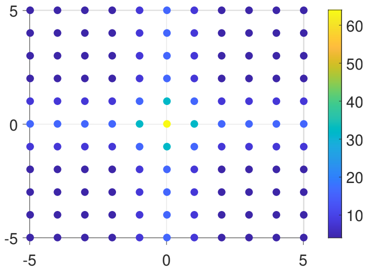

Fig. 2. Redundancies among the coarray sensors lying in the x-y plane ($z = 0$). Since there are 64 actual sensors, so there are 64 virtual coarray sensors at the origin owing to the self differences. Similarly, the colour of the dots indicate the number of redundancies in other locations. These redundancies (along with the redundancies in the other planes) are the reason that the DOF of the coarray is 1331 and not $64^2 = 4096$.

2) 3D Coarray Signal Model and Spatial Smoothing: Now that the structure of the difference coarray is known, we need to figure out the signal received by the coarray. Since the elements in $\mathbf{R}$ depends on the coarray, vectorizing it gives

$$\begin{aligned}\mathbf{z} = \text{vec}(\mathbf{R}) &= \text{vec}\left(\sum_{l=1}^{L} p_l \mathbf{a}(\theta_l,\phi_l)\mathbf{a}^H(\theta_l,\phi_l) + \sigma_\eta^2 \mathbf{I}_N\right) \\ &= (\mathbf{A}^* \odot \mathbf{A})\mathbf{p} + \sigma_\eta^2 \text{vec}(\mathbf{I}_N) \\ &= \bar{\mathbf{A}}\mathbf{p} + \sigma_\eta^2 \mathbf{i}. \end{aligned} \tag{9}$$

Here $\bar{\mathbf{A}} = (\mathbf{A}^* \odot \mathbf{A}) = [\bar{\mathbf{a}}(\theta_1,\phi_1), \cdots, \bar{\mathbf{a}}(\theta_L,\phi_L)]$ acts as the coarray steering matrix, $\mathbf{p} = [p_1, p_2, \ldots, p_L]$ is the vector of signal powers and $\mathbf{i} = \text{vec}(\mathbf{I}_N)$. The coarray steering vector corresponding to the l^{th} source can be expressed as

$$\bar{\mathbf{a}}(\theta_l,\phi_l) = \mathbf{a}^*(\theta_l,\phi_l) \otimes \mathbf{a}(\theta_l,\phi_l). \tag{10}$$

We can see that after removing the redundant rows, the length of the coarray steering vector is the same as the number of sensors (D) in the difference coarray. Comparing with (2), (9) can be seen as the coarray signal model. Since the equivalent signal for the coarray is the vector $\mathbf{p}$ containing the powers of the signal, the coarray signal model is a single snapshot model. As such, the rank of the coarray covariance matrix (CCM) $[\mathbf{z}\mathbf{z}^H]$ is 1. High resolution subspace-based DOA estimation methods such as MUSIC operate by extracting the noise subspace of the covariance matrix by performing eigen-value decomposition (EVD). Thus, we cannot apply these methods directly to the coarray and need to recover the rank of the CCM before subspace based algorithms can be applied to the coarray model. To do this, we perform a spatial smoothing type operation [2], [19]. First, we once again remind that the difference coarray has virtual sensors located in three dimensions at $(\{-M,\ldots,M\}d_x \oplus \{-M,\ldots,M\}d_y \oplus \{-M,\ldots,M\}d_z)$ where $M = N_2(N_1+1) - 1$. We can now divide this coarray into $(M+1)^3$ overlapping 3D subarrays, each with $(M+1)^3$ coarray sensors. These subarrays have sensors located at

$$\begin{aligned} &(-i+1+n)d_x, \quad n = 0,1,\ldots,M \\ &(-j+1+n)d_y, \quad n = 0,1,\ldots,M \\ &(-k+1+n)d_z, \quad n = 0,1,\ldots,M \end{aligned}$$

where $i,j,k \in \{1,\ldots,(M+1)\}$. Let the vectorized signal captured by the q^{th} subarray be given by $\mathbf{z}_q$. Then, the covariance matrix of the q^{th} subarray is $\mathbf{R}_q = \mathbf{z}_q\mathbf{z}_q^H$. Taking the average of the covariance matrices of the $Q = (M+1)^3$ subarrays gives

$$\mathbf{R}_{\text{SS}} = \frac{1}{(M+1)^3} \sum_{q=1}^{(M+1)^3} \mathbf{R}_q \tag{11}$$

The spatially smoothed $\mathbf{R}_{\text{SS}}$ has a rank of $(M+1)^3$. So, rank recovery of the CCM through the spatial smoothing operation reduced the DOF of the difference coarray from $(2N_2(N_1+1)-1)^3$ to $(M+1)^3 = (N_2(N_1+1))^3$. Taking the average of $(M+1)^3$ matrices is computationally very expensive. So, noting the three-fold toeplitz structure of the CCM, we propose an additional efficient method to construct a full rank CCM directly form the elements of coarray vector $\mathbf{z}$ as laid out in theorem 1.

Theorem 1. *The three-fold toeplitz matrix $\mathbf{T}$ defined as*

$$\mathbf{T} = \begin{bmatrix} \mathbf{T}_0 & \mathbf{T}_1^H & \cdots & \mathbf{T}_M^H \\ \mathbf{T}_1 & \mathbf{T}_0 & \cdots & \mathbf{T}_{(M-1)}^H \\ \vdots & \vdots & \ddots & \vdots \\ \mathbf{T}_M & \mathbf{T}_{(M-1)} & \cdots & \mathbf{T}_0 \end{bmatrix}, \tag{12}$$

is hermitian and $\mathbf{R}_{\text{SS}} = \mathbf{T}^2/(M+1)^3$. Here, each block in $\mathbf{T}$ is a two-fold toeplitz matrix given by

$$\mathbf{T}_x = \begin{bmatrix} \mathbf{T}_{x0} & \mathbf{T}_{x1}^H & \cdots & \mathbf{T}_{xM}^H \\ \mathbf{T}_{x1} & \mathbf{T}_{x0} & \cdots & \mathbf{T}_{x(M-1)}^H \\ \vdots & \vdots & \ddots & \vdots \\ \mathbf{T}_{xM} & \mathbf{T}_{x(M-1)} & \cdots & \mathbf{T}_{x0} \end{bmatrix}$$

and each block in $\mathbf{T}_x$ is a toeplitz matrix made up of the elements of $\mathbf{z}$ as (here $[\mathbf{z}]_{x,y,z}$ is the element in $\mathbf{z}$ corresponding to the $(x,y,z)^{th}$ coarray sensor)

$$\mathbf{T}_{xy} = \begin{bmatrix} [\mathbf{z}]_{x,y,0} & [\mathbf{z}]_{x,y,-1} & \cdots & [\mathbf{z}]_{x,y,-M} \\ [\mathbf{z}]_{x,y,1} & [\mathbf{z}]_{x,y,0} & \cdots & [\mathbf{z}]_{x,y,-(M-1)} \\ \vdots & \vdots & \ddots & \vdots \\ [\mathbf{z}]_{x,y,M} & [\mathbf{z}]_{x,y,(M-1)} & \cdots & [\mathbf{z}]_{x,y,0} \end{bmatrix}$$

Proof. From (9), $\mathbf{z}$ is hermitian symmetric i.e. $\mathbf{z} = \mathbf{J}\mathbf{z}^*$ where $\mathbf{J}$ is the anti-diagonal matrix with ones along the anti-diagonal and zeros elsewhere.
Now, The hermitian of $\mathbf{T}_{xy}$ can be written as

$$\mathbf{T}_{xy}^H = \begin{bmatrix} [\mathbf{z}]_{x,y,0}^* & [\mathbf{z}]_{x,y,1}^* & \cdots & [\mathbf{z}]_{x,y,M}^* \\ [\mathbf{z}]_{x,y,-1}^* & [\mathbf{z}]_{x,y,0}^* & \cdots & [\mathbf{z}]_{x,y,(M-1)}^* \\ \vdots & \vdots & \ddots & \vdots \\ [\mathbf{z}]_{x,y,-M}^* & [\mathbf{z}]_{x,y,-(M-1)}^* & \cdots & [\mathbf{z}]_{x,y,0}^* \end{bmatrix}$$

Since $\mathbf{z} = \mathbf{J}\mathbf{z}^*$, every element in $\mathbf{T}_{xy}^H$ can be replaced with corresponding elements in $\mathbf{z}$ which will result in $\mathbf{T}_{xy}^H = \mathbf{T}_{xy}$. Therefore, $\mathbf{T}^H = \mathbf{T}$. Now, from (11), we can define $\mathbf{R}_{\text{SS}}$ as

$$\mathbf{R}_{\text{SS}} = \frac{1}{(M+1)^3} \sum_{q=1}^{(M+1)^3} \mathbf{J}_q \mathbf{z}\mathbf{z}^H \mathbf{J}_q^H \tag{13}$$

where $\mathbf{J}_q \in \{0,1\}^{(M+1)^3 \times D}$ is a selection matrix which selects the elements that make up the different subarrays from the coarray signal vector $\mathbf{z}$. Also, from the definition of $\mathbf{T}$ in (12), it can be written as

$$\mathbf{T} = \begin{bmatrix}\mathbf{J}_1\mathbf{z} & \mathbf{J}_2\mathbf{z} & \cdots & \mathbf{J}_{(M+1)^3}\mathbf{z}\end{bmatrix}. \tag{14}$$

Now, squaring the matrix $\mathbf{T}$, we get

$$\begin{aligned}\mathbf{T}^2 &= \mathbf{T}\mathbf{T}^H \\ &= \mathbf{J}_1\mathbf{z}(\mathbf{J}_1\mathbf{z})^H + \mathbf{J}_2\mathbf{z}(\mathbf{J}_2\mathbf{z})^H \\ &\qquad + \cdots + \mathbf{J}_{(M+1)^3}\mathbf{z}\big(\mathbf{J}_{(M+1)^3}\mathbf{z}\big)^H \\ &= \sum_{q=1}^{(M+1)^3} \mathbf{J}_q\mathbf{z}\mathbf{z}^H\mathbf{J}_q^H \\ &= (M+1)^3\mathbf{R}_{\text{SS}}\end{aligned} \tag{15}$$

which is equal to $\mathbf{R}_{\text{SS}} = \mathbf{T}^2/(M+1)^3$ which concludes the proof. □

From theorem 1, the eigenvectors of $\mathbf{T}$ span the same subspace as that of $\mathbf{R}_{\text{SS}}$. So, we can apply coarray MUSIC algorithm to $\mathbf{T}$ whose spectrum is given by

$$S(\theta,\phi) = \frac{1}{\left(\bar{\mathbf{a}}_1^H(\theta,\phi)\mathbf{E}_\eta\mathbf{E}_\eta^H\bar{\mathbf{a}}_1(\theta,\phi)\right)}, \tag{16}$$

where $\bar{\mathbf{a}}_1(\theta,\phi)$ is the steering vector of the first subarray corresponding to $i=j=k=1$ and $\mathbf{E}_\eta$ is the $(M+1)^3 \times ((M+1)^3 - L)$ noise subspace of $\mathbf{T}$. The spectrum $S(\theta,\phi)$ gives peaks at the location of the DOAs of the sources. So, using only N sensors, we will theoretically be able to estimate the DOAs of $((M+1)^3 - 1)$ sources using the proposed array. In practical situations, the actual array covariance matrix $\mathbf{R}$ is not available, so we use the sample covariance matrix $\hat{\mathbf{R}}$ (which is the maximum likelihood estimate of $\mathbf{R}$ [1]) as $\frac{1}{\Gamma}\sum_{t=1}^{\Gamma}\mathbf{x}(t)\mathbf{x}^H(t)$ where Γ is the total number of snapshots.

III. Cramer-Rao Bound (CRB) Analysis

In [20], a closed-form expression of the CRB is derived for the case of 3D sensor array made from ULA branches. However, the expression derived is only applicable to the case when the number of sources is less than the number of sensors. It fails for the underdetermined case. In [21], the CRB expression was derived for the underdetermined case but it is only applicable for linear arrays. In this section, we derive the CRB for signal model (2) which will be applicable to underdetermined DOA estimation using sparse 3D arrays. Using (2), the vector of the parameters that are being estimated is given by

$$\boldsymbol{\gamma} = [\theta_1, \cdots, \theta_L, \phi_1, \cdots, \phi_L]^T, \tag{17}$$

Now, the $(u,v)^{th}$ term of the Fisher Information Matrix (FIM) is given as [22]

$$\begin{aligned}\text{FIM}_{uv} &= \Gamma\,\text{tr}\left[\frac{\partial\mathbf{R}}{\partial\gamma_u}\mathbf{R}^{-1}\frac{\partial\mathbf{R}}{\partial\gamma_v}\mathbf{R}^{-1}\right] &(18)\\ &= \Gamma\left[\frac{\partial\mathbf{z}}{\partial\gamma_u}\right]^H(\mathbf{R}^T\otimes\mathbf{R})^{-1}\frac{\partial\mathbf{z}}{\partial\gamma_v}. &(19)\end{aligned}$$

By denoting the derivatives of $\mathbf{z}$ with respect to $\boldsymbol{\gamma}$ as $\frac{\partial\mathbf{z}}{\partial\boldsymbol{\gamma}} = \left[\frac{\partial\mathbf{z}}{\partial\theta_1}, \cdots, \frac{\partial\mathbf{z}}{\partial\theta_L}, \frac{\partial\mathbf{z}}{\partial\phi_1}, \cdots, \frac{\partial\mathbf{z}}{\partial\phi_L}\right]$, the FIM can be written more compactly as

$$\text{FIM} = \left[\frac{\partial\mathbf{z}}{\partial\boldsymbol{\gamma}}\right]^H(\mathbf{R}^T\otimes\mathbf{R})^{-1}\frac{\partial\mathbf{z}}{\partial\boldsymbol{\gamma}}. \tag{20}$$

Using (9), the derivative in (20) can be written as

$$\frac{\partial\mathbf{z}}{\partial\boldsymbol{\gamma}} = \left[\bar{\mathbf{A}}_{\text{d}\theta}\mathbf{P}, \bar{\mathbf{A}}_{\text{d}\phi}\mathbf{P}\right], \tag{21}$$

where $\mathbf{P} = \text{diag}(\mathbf{p})$, $\bar{\mathbf{A}}_{\text{d}\theta} = \mathbf{A}_{\text{d}\theta}^* \odot \mathbf{A} + \mathbf{A}^* \odot \mathbf{A}_{\text{d}\theta}$ and $\bar{\mathbf{A}}_{\text{d}\phi} = \mathbf{A}_{\text{d}\phi}^* \odot \mathbf{A} + \mathbf{A}^* \odot \mathbf{A}_{\text{d}\phi}$. Further,

$$\mathbf{A}_{\text{d}\theta} = \left[\frac{\partial\mathbf{a}(\theta_1,\phi_1)}{\partial\theta_1}, \frac{\partial\mathbf{a}(\theta_2,\phi_2)}{\partial\theta_2}, \cdots, \frac{\partial\mathbf{a}(\theta_L,\phi_L)}{\partial\theta_L}\right], \tag{22}$$

$$\mathbf{A}_{\text{d}\phi} = \left[\frac{\partial\mathbf{a}(\theta_1,\phi_1)}{\partial\phi_1}, \frac{\partial\mathbf{a}(\theta_2,\phi_2)}{\partial\phi_2}, \cdots, \frac{\partial\mathbf{a}(\theta_L,\phi_L)}{\partial\phi_L}\right]. \tag{23}$$

Now, because $\mathbf{R}$ is positive definite, $(\mathbf{R}^T\otimes\mathbf{R})^{-1/2}$ exits. Let $\mathbf{F} = [\mathbf{F}_\theta, \mathbf{F}_\phi]$ where

$$\mathbf{F}_\theta = (\mathbf{R}^T\otimes\mathbf{R})^{-1/2}\bar{\mathbf{A}}_{\text{d}\theta}\mathbf{P}, \tag{24}$$

$$\mathbf{F}_\phi = (\mathbf{R}^T\otimes\mathbf{R})^{-1/2}\bar{\mathbf{A}}_{\text{d}\phi}\mathbf{P}. \tag{25}$$

It can be seen that $\text{FIM} = \Gamma(\mathbf{F}^H\mathbf{F})$. So, finally,

$$\text{CRB}(\gamma_i) = \left[\text{FIM}^{-1}\right]_{ii} = \frac{1}{\Gamma}\left[(\mathbf{F}^H\mathbf{F})^{-1}\right]_{ii} \tag{26}$$

IV. Simulation Results

In this section, we illustrate the advantages of the proposed array by performing underdetermined DOA estimation. For the simulations, we choose a 3D nested array with $N_1 = N_2 = 2$ as shown in Figure 1(c). The total number of sensors in the array is $(N_1+N_2)^3 = 64$. The DOF of the coarray after spatial smoothing operation is 216.

1) Coarray MUSIC Spectrum: We assume that $L = 72$ sources, all having unit power, impinge on the array with directions given by the (θ_l, ϕ_l) pairs as $\left\{\left(30^\circ + (i-1)\frac{120^\circ}{7}, 30^\circ + (j-1)\frac{300^\circ}{8}\right), i = 1,2,\ldots,8, j = 1,2,\ldots,9\right\}$. The 3D coarray MUSIC spectrum is shown in Figure 3. We can see that although the original array only has 64 sensors, it is providing distinct peaks for the 72 source DOAs. The peaks become refined and the quality of the spectrum improves with increasing number of snapshots. This is a huge advantage as traditional 3D arrays with 64 sensors are not capable of localizing more than 63 sources and their performance severely degrades as they reach this theoretical limit.

2) RMSE performance versus SNR and snapshots: In this section, we analyze the DOA estimation performance of the 3D nested array while varying the SNR and the number of snapshots. The performance metric is chosen to be the root-mean-square-error (RMSE) which is defined as $\sqrt{\frac{1}{WL}\sum_{w=1}^{W}\sum_{l=1}^{L}\left(\hat{\phi}_{lw} - \phi_l\right)^2}$ for the azimuth estimation (W denotes the total number of Monte-Carlo runs and $\hat{\phi}_{lw}$ denotes

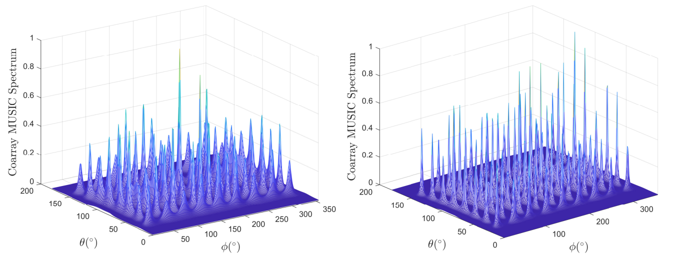

(a) No. of snapshots = 500, SNR = 10 dB (b) No. of snapshots = 2000, SNR = 10 dB

Fig. 3. Normalized 3D Coarray MUSIC spectrum showing the DOA estimate of 72 sources using a 64 sensor 3D nested array. Note that the peaks become more prominent as the number of snapshots increases.

the estimate of the azimuth angle of the l^{th} source in the w^{th} Monte-Carlo run). RMSE for elevation estimation can be defined in a similar manner. The DOAs of the sources are the same as before. As a benchmark, we have compared the performance of the proposed 3D nested array with a Uniform Cube array having 125 sensors. Figure 4 shows the RMSE performance. For each point on the plot, the total number of independent runs was set to $W = 500$. In each of these runs, the signal and noise vectors were randomly generated. As the SNR and the number of snapshots increases, the error decreases. In fact, even though the number of sensors in our array is much less than the benchmark, the DOA estimation performance starts to match the level of the benchmark for higher values of SNR and snapshots.

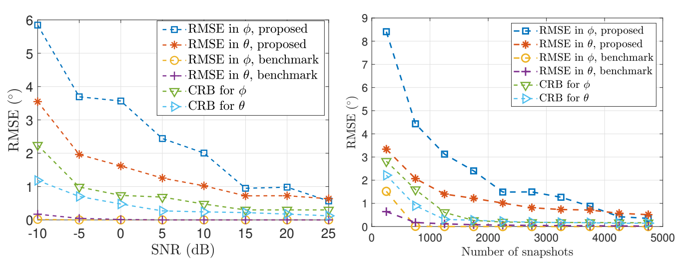

(a) No. of snapshots = 1000 (b) SNR = 5 dB

Fig. 4. RMSE performance of 3D Coarray MUSIC for underdetermined DOA estimation of 72 sources versus SNR and number of snapshots. The benchmark was chosen as a 125 sensor uniform cube array and direct MUSIC was used to calculate the benchmark DOAs.

V. Conclusion

A 3D sparse nested sensor array configuration is presented that is capable of performing underdetermined source localization. The 3D nested array is designed is such a manner that its difference coarray is hole free and as such subspace-based method can be applied after perfoming a 3D spatial smoothing type operation to construct the coarray covariance matrix. Comparing the performance of the proposed configuration with dense arrays shows its advantages and the usefulness. In the future, a general lattice based 3D nested array configuration will be studied. Another important direction would be to use the proposed array for beamforming applications and wideband sources.

References

[1] H. L. Van Trees, *Optimum array processing: Part IV of Detection, Estimation, and Modulation Theory*. John Wiley & Sons, 2004.
[2] P. Pal and P. P. Vaidyanathan, "Nested arrays: A novel approach to array processing with enhanced degrees of freedom," *IEEE Trans. Signal Process.*, vol. 58, no. 8, pp. 4167–4181, 2010.
[3] C.-L. Liu and P. Vaidyanathan, "Remarks on the spatial smoothing step in coarray MUSIC," *IEEE Signal Process. Lett.*, vol. 22, no. 9, pp. 1438–1442, 2015.
[4] ——, "Super nested arrays: Linear sparse arrays with reduced mutual coupling—Part I: Fundamentals," *IEEE Trans. Signal Process.*, vol. 64, no. 15, pp. 3997–4012, 2016.
[5] J. Liu, Y. Zhang, Y. Lu, S. Ren, and S. Cao, "Augmented nested arrays with enhanced DOF and reduced mutual coupling," *IEEE Trans. Signal Process.*, vol. 65, no. 21, pp. 5549–5563, 2017.
[6] Z. Zheng, W.-Q. Wang, Y. Kong, and Y. D. Zhang, "MISC array: A new sparse array design achieving increased degrees of freedom and reduced mutual coupling effect," *IEEE Trans. Signal Process.*, vol. 67, no. 7, pp. 1728–1741, 2019.
[7] S. Ren, W. Dong, X. Li, W. Wang, and X. Li, "Extended nested arrays for consecutive virtual aperture enhancement," *IEEE Signal Process. Lett.*, vol. 27, pp. 575–579, 2020.
[8] S. K. Yadav and N. V. George, "Fast direction-of-arrival estimation via coarray interpolation based on truncated nuclear norm regularization," *IEEE Trans. Circuits Syst. II, Exp. Brief*, vol. 68, no. 4, pp. 1522–1526, 2020.
[9] P. Pal and P. Vaidyanathan, "Nested arrays in two dimensions, Part I: Geometrical considerations," *IEEE Trans. Signal Process.*, vol. 60, no. 9, pp. 4694—4705, 2012.
[10] C.-L. Liu and P. P. Vaidyanathan, "Hourglass arrays and other novel 2-D sparse arrays with reduced mutual coupling," *IEEE Trans. Signal Process.*, vol. 65, no. 13, pp. 3369–3383, 2017.
[11] X. Yang, Y. Wang, and P. Chargé, "Hole locations and a filling method for coprime planar arrays for DOA estimation," *IEEE Commun. Lett.*, vol. 25, no. 1, pp. 157–160, 2021.
[12] W. Zheng, X. Zhang, and H. Zhai, "Generalized coprime planar array geometry for 2-D DOA estimation," *IEEE Commun. Lett.*, vol. 21, no. 5, pp. 1075–1078, 2017.
[13] H. Zheng, C. Zhou, Y. Gu, and Z. Shi, "Two-dimensional DOA estimation for coprime planar array: A coarray tensor-based solution," in *Proc. IEEE Int. Conf. Acoust., Speech Signal Process.*, 2020, pp. 4562–4566.
[14] J. Shi, G. Hu, X. Zhang, F. Sun, and H. Zhou, "Sparsity-based two-dimensional doa estimation for coprime array: From sum–difference coarray viewpoint," *IEEE Trans. Signal Process.*, vol. 65, no. 21, pp. 5591–5604, 2017.
[15] G. Qin, M. G. Amin, and Y. D. Zhang, "DOA estimation exploiting sparse array motions," *IEEE Trans. Signal Process.*, vol. 67, no. 11, pp. 3013–3027, 2019.
[16] S. Li and X.-P. Zhang, "Dilated arrays: A family of sparse arrays with increased uniform degrees of freedom and reduced mutual coupling on a moving platform," *IEEE Trans. Signal Process.*, 2021.
[17] S. K. Yadav and N. V. George, "Underdetermined direction-of-arrival estimation using sparse circular arrays on a rotating platform," *IEEE Signal Process. Lett.*, vol. 28, pp. 862–866, 2021.
[18] C. Li, L. Gan, and C. Ling, "3D coprime arrays in sparse sensing," in *Proc. IEEE Int. Conf. Acoust., Speech Signal Process.*, 2019, pp. 4200–4204.
[19] P. Pal and P. Vaidyanathan, "Nested arrays in two dimensions, Part II: Application in two dimensional array processing," *IEEE Trans. Signal Process.*, vol. 60, no. 9, pp. 4706–4718, 2012.
[20] D. T. Vu, A. Renaux, R. Boyer, and S. Marcos, "A cramér rao bounds based analysis of 3d antenna array geometries made from ula branches," *Multidimensional Syst. Signal Process.*, vol. 24, no. 1, pp. 121–155, 2013.
[21] M. Wang and A. Nehorai, "Coarrays, music, and the cramér–rao bound," *IEEE Trans. Signal Process.*, vol. 65, no. 4, pp. 933–946, 2016.
[22] S. M. Kay, *Fundamentals of statistical signal processing: estimation theory*. Prentice-Hall, Inc., 1993.